Finite Element Study of the Effect of Structural Modifications on Structure-Borne Vehicle Interior Noise

V. B. GEORGIEV and V. V. KRYLOV *)

Department of Aeronautical and Automotive Engineering,
Loughborough University,
Loughborough, Leicestershire, LE11 3TU, UK

*) Corresponding author: V.V.Krylov@lboro.ac.uk

Abstract: This paper presents the results of the numerical investigation of structure-borne vehicle interior noise in a simplified model of vehicle compartment. The aim of the paper is to analyse the effects of different variations of certain geometrical and material parameters of vehicle structure on structural-acoustic frequency response functions. It has been found that geometrical modifications have little influence on the structural natural frequencies. However, they strongly affect the acoustic natural frequencies and normal modes as well as the resulting sound pressure responses. The increase in thickness of the bottom plate suppresses the sound pressure responses very efficiently. However, variations of material characteristics of wind- and back-screen do not have much influence on the interior noise.

Keywords: Structure-borne vehicle interior noise; Finite element analysis; Simplified vehicle models; Structural-acoustic interaction.

1. INTRODUCTION

Numerical methods of studying structural vibrations and structural-acoustic interactions are used widely by car developers to predict and reduce structure-borne vehicle-interior noise. Modern finite element (FE) techniques can describe very complex vehicle structures in great detail, which leads to numerical results that are comparable with experimental ones (see, for example, Nefske et al. (1982), Sung and Nefske (1984), Petyt et al. (1976), Lim (2000)). However, in many cases the use of very complex numerical models of vehicle structures does not help a developer to better understand specific physical mechanisms of structure-borne interior noise typical for the model under consideration. In this regard, investigation of *simplified* structural models by FE methods could provide an additional very useful and practically important insight into the problem. Futhermore, the use of simplified models for numerical investigations can give the opportunity for a quick change of the model parameters and for immediate estimate of the results of alteration. Thus, such simplified models can assist in identifying the most important parameters influencing generation of structure-borne interior noise in vehicle compartments.

One of the simplest and widely used structural-acoustic models is a mostly rigid rectangular box with only one vibrating wall. One can obtain an exact analytical solution for such a model, and the existence of such a solution has proven to be very useful to achieve better understanding of structural-acoustic interaction (Lyon (1963), Pretlove (1965, 1966)). Vibrations of some other simple geometrical structures, such as all-flexible rectangular boxes that can be used to emulate real vehicle bodies, have been

investigated analytically using approximate approaches (Fulford and Petersson (2000), Liang and Petersson (2001)).

Recently, a more complex but still rather simple model of vehicle body structure built up of a non-circular cylindrical shell with two rigid side walls has been investigated both theoretically and experimentally (Krylov (2002), Krylov et al. (2003), Georgiev et al. (2004)). The main advantage of this structure was the ability of obtaining an approximate analytical solution for sound pressure in the vehicle interior as a function of the model parameters, road irregularity, vehicle speed, properties of vehicle suspensions, etc.

Note that some authors utilized simple structural models, mainly box-type structures, to verify different optimization procedures for noise reduction (see, for example, Marburg et al. (2002), Luo and Gea (2003)). In this regard, simple models assisted in a quicker estimation of the proposed design modifications from the point of view of noise reduction.

In spite of some important advances achieved using the above-mentioned simple structural models, there is still a wide gap between such simple models and highly detailed models of real vehicle prototypes analysed by car manufacturers by means of specially developed commercial software based on finite or boundary element techniques. The simplest box-type models, although very imprecise, are more or less well understood, whereas real vehicle models, having rather complex geometrical forms and material properties, are very difficult to interpret and, as a result, very difficult to modify in a desirable way to reduce generated structure-borne noise.

In the light of the above, the main aim of the present paper is to carry out a parametric study of a simplified compartment model of medium complexity in order to

bridge the currently existing gap between the simplest box-type models and much more detailed commercial models of real vehicles. A number of essential vehicle parameters are being considered, including different angels of windshield, different lengths and thickness of certain panels, and different materials. The objective of this parametric study is to investigate the influence of gradual changes in different parameters of a vehicle structure on structure-borne interior noise. The developed approach and the obtained results would be of interest to specialists in vehicle refinement working on optimisation of structural design from the point of view of reduction of structure-borne vehicle interior noise.

2. DESCRIPTION OF THE BASE MODEL

The base model represents a simplified replica of a vehicle compartment made of welded steel plates (see Fig. 1(a)). The overall dimensions of the model are 2, 1.5 and 1.4 m respectively in X (longitudinal), Y (vertical) and Z (lateral) directions. The material parameters of the steel plates used in the model are as follows: Young's modulus $E = 2.10^{11}, N/m^2$, Poisson's ratio $\nu = 0.31$ and the mass density $\rho = 7950$ kg/m^3. The thickness of all plates is 0.005 m, which results in the model's fundamental structural frequency of 18 Hz. This matches fundamental frequencies of typical car bodies, that are in the range of 5–20 Hz. The acoustic parameters of the air are: speed of sound 331.3 m/s and the mass density 1.29 kg/m^3, which results in the first acoustic resonance frequency in the above compartment at about 103 Hz. The material loss factors were assumed to be 1% and 3% respectively for acoustic and structural sub-systems.

In the present study, finite element packages MSC.Nastran and MSC.Patran, version 2006, have been used for numerical analysis of structure-borne interior noise in the above-mentioned simplified vehicle model. The numbers of fully coupled structural and acoustic finite elements and element nodes were nearly the same for all variations of the model parameters. For the structural part of the analysis, “CQUAD” finite elements were used, whereas for the acoustic part, “CHEXA” finite elements were employed. The mesh size was consistent with the maximum frequency range of interest, which was 500 Hz (an acoustic wavelength of 0.6626 m). Note that the recommended minimum number of finite elements per wavelength is six. This means that the finite element size must be less than 0.11 m. In the light of this, the size of 0.05 m has been chosen that corresponds to about 12 finite elements per an acoustic wavelength. Thus, fot the base model 16567 acoustic and 721 structural finite elements have been used. The numbers of acoustic and structural finite elements in the modified models were close to those for the base one.

Simply supported boundary conditions were imposed at the bottom corners of the models. Although these boundary conditions do not represent boundary conditions imposed on a real vehicle, they can be used for numerical calculations as they restrict only the rigid body motion of the model. It can be shown that the rigid body motion of a structural-acoustic system does not affect sound generation inside the cavity (Georgiev et al. (2004)).

Note that for all changes of structural parameters analysed in this work, the input and output points, corresponding to the positions of a set of disturbing forces exciting structural vibrations and a receiver respectively, remained the same. This provided a

meaningful comparison of the results obtained for the models with different modifications.

The model structure was excited by a harmonic force of variable frequency and of the fixed amplitude of 200 N. The force was applied to the structure at the four points located on the bottom plate, having the coordinates: (1.4; 0; 1.35), (1.4; 0; 0.25), (0.5; 0; 0.25), and (0.5; 0; 1.35), where all coordinates are in meters, measured from the origin located at the bottom left corner (see Figure 1). The coordinates of the receiver for all model's variations corresponded to the driver's ear position - (0.962; 0.836; 0.45), and to the passenger's ear position - (1.452; 0.87; 0.45).

3. EFFECTS OF GEOMETRICAL VARIATIONS

3.1 Variations in the Windscreen Panel and in the Top Panel

In order to study the effect of windscreen geometrical parameters on sound pressure frequency response, three different variations have been considered (see Fig. 1(b)). The main change was associated with the location of the top left point of the model, as can be seen in Fig. 1(b). The X coordinate of the point was altered by 0.1 m. For the sake of simplicity, the base model (Fig. 1(a)) will be referred to as model 1. The coordinates of the point under consideration for this model are (0.9; 1.0; 0). The second variation will be referred to as model 2, with the coordinates of the top left point being (0.8; 1.0; 0). And for the last variation, model 3, the coordinates of the same point are (0.7; 1.0; 0).

Note that the above change in the longitudinal coordinate of the top left point of the model (with the step of 10 cm) has twofold effect on the structural modifications.

Firstly, the angle between the windscreen and the dashboard plate has been changed from 23.95° in model 1 through 26.55° in model 2 to 29.74° in the last model 3. Secondly, the length of the top panel changed in X direction from 0.6 m in model 1, through 0.7 m in model 2 to 0.8 m in model 3. Therefore, the change in the simulated sound pressure responses was induced by the change of both the length of the top and windscreen plates and by the angle between the windscreen and dashboard plates.

Figures 2(a) and 3(a) show the comparisons between the sound pressure responses calculated at the driver's ear position respectively for models 1 and 2 (Fig. 2(a)) and for models 1 and 3 (Fig. 3(a)). Figures 2(b) and 3(b) represent the pressure differences between the sound pressure responses for the same models. Analysing the graph in Fig. 2(b), one can notice two strong difference peaks at about 165 Hz and 270 Hz caused by strong anti-resonances in model 2 at these frequencies. Other amplitude difference peaks are those at 120 Hz and at 200 Hz. Some of the pressure differences go above 20 dB. At the rest of the frequency contents the difference varies around ±5 dB. In contrast to Fig. 2(b), in Fig. 3(b) there is one strong difference peak at about 99 Hz, but the overall pressure difference between models 1 and 3 varies between -5 dB to +10 dB.

In the light of above, one can conclude that the change from model 1 to model 2 leads to noticeable difference between the sound pressure responses at the driver's ear position. This difference is fairly visible at about 120, 165 and 270 Hz, where the pressure differences reach to about 20 dB. Note that these differences are caused by the fact that the sound pressure response in model 2 has strong anti-resonances at these frequencies. The subsequent alteration, from model 1 through model 2 to model 3, does not lead to drastic changes in the sound pressure response at the driver's ear position and results only in a small average increase in sound pressure level.

Note that for both cases, in Fig. 2(b) and in Fig. 3(b), the most noticeable changes (e.g. at about 99, 103, 165, 200, and 270 Hz) are associated with acoustically dominated resonances. This could suggest that small changes in the longitudinal coordinate of the top left edge of the base model do not affect significantly structurally dominated resonant peaks of the sound pressure responses calculated at the driver's ear position. In the same time, the acoustically dominated sound pressure resonances are considerably influenced by these changes, mainly because they change the locations of nodal planes.

3.2 Variations of the Model Height

The structural modifications in this case can be seen in Fig. 1(c). The alteration of the model's height is related to the change of the wind-, back-screen and top panel length. Thus, the sound pressure differences calculated in this case are due to the above mentioned geometrical variations. Figure 4(a) shows the sound pressure responses calculated at the driver's ear position for three different heights of the base model. The solid, dash-dotted and dashed curves in Fig. 4(a) represent respectively the sound pressure responses in the base model (with a height of: h = 1 m) and in the two modified models (with h = 0.9 m and h = 1.1 m). These modifications in height of the model (about 10 %) lead to the following changes: in the length of the windscreen panel: 0.9 m at h = 1 m, 0.67 m at h = 0.9 m, and 1.12 m at h = 1.1 m. The same height modifications cause the following alterations: in the length of the back screen panel, respectively – 0.58 m, 0.39 m, and 0.78 m; and in the length of the top plate – 0.7 m, 1.07 m, and 0.33 m.

Figure 4(b) shows the pressure differences between the sound pressure responses of the base model (h = 1 m) and: the first modification (h = 1.1 m), called Diff 1, and the

second modification (h = 0.9 m), called Diff 2. Similarly to the previous section, the sound pressure differences have some large peaks, such as those at about 210, 350 and 440 Hz, and the rest of the plots vary in the interval of ±10 dB. It is noticeable that the large peaks for both graphs in Fig. 4(b) appear in the area above 200 Hz. In particular, the resonant peak at about 210 Hz is strongly affected by the change in the height of the base model. Obviously, the modifications shift slightly the resonant peak, and in the modified models an anti-resonance appears at the same frequency where there was formerly a resonance - at about 210 Hz (see Fig. 4(a)). Similarly, if the height of the model is increased to h = 1.1 m, the resonance at about 350 Hz disappears as an anti-resonance comes into sight in the modified model. Thus, an increase of 10 % in the height leads to about 34 dB reduction at about 350 Hz.

3.3 Variations of the Model Length

The structural variations in this case can be seen in Fig. 1(d). As a result of these modifications, the lengths of the top and of the bottom panels are changed, whereas all other geometrical parameters of the model stay the same. Figure 5(a) shows the sound pressure responses calculated at the driver's ear position for three different variations of the overall dimension in X direction. The length of the base model is L = 2.0 m, whereas the other two models have lengths of about 5 % less and more, L = 1.9 m and L = 2.1 m, respectively. Figure 5(b) shows the calculated pressure differences between the base model and the two modified models. In particular, curve Diff 1 corresponds to the pressure difference between the base model (L = 2 m) and the model with L = 2.1 m, whereas curve Diff 2 represents the difference between the base model (L = 2 m) and the model with L = 1.9 m.

Analysing Fig. 5(b), one can notice certain large positive peaks at about 130, 180, 370 and 430 Hz, where the structural modifications of the base model reduced the sound pressure responses at these frequencies. On the other hand, the substantial negative peaks at around 100, 170 and 270 Hz show that the above modifications increased the sound pressure responses at the respective frequencies. The sound pressure difference varies at the rest of the frequency contents. The interval below the first acoustic natural frequency, at about 98 Hz, can be characterised by a pressure difference less than 12-13 dB.

A common feature of all structural modifications considered so far is the presence of strong pressure difference peaks (30-40 dB) in the area above the first acoustic natural frequency. In the same time, in the frequency range below the first acoustic resonance, the pressure differences between the models stay relatively moderate (10-13 dB). Thus, the considered structural modifications that involve changes in the model's geometrical parameters for constant thickness of the constitutive plates can cause significant increases or decreases in sound pressure responses at certain frequencies. In this regard, it is interesting to study the effect of plate thickness (or plate mass) variations in the models of the same shape, which follows next.

3.4 Variations in Thickness of the Bottom Plate

In this case, it is anticipated that frequencies of most of the structural resonant peaks will be affected, whereas frequencies of the acoustic resonant peaks will stay unchanged. Figure 6, (a) and (b), shows the sound pressure responses calculated for the base model (see Fig. 1(a)) at the driver's and passenger's ear positions respectively. The

thickness of the bottom plate was varied and had the values of 0.002, 0.005 and 0.008 m.

The results in Fig. 6 show that the increase in thickness of the bottom plate leads to large overall reductions in the sound pressure responses calculated at both driver's and passenger's ear positions. This is in agreement with the results shown for a simpler analytical model (Krylov (2002) following from the fact that a structural Green's function is inversely proportional to the mass of a structure. As it was anticipated, some of the observed peaks become shifted in frequency as a result of thickness modifications, and some remain stationary, although the amplitudes of most of the peaks change as a rule. Apparently, in the latter case the corresponding resonant frequencies are acoustically dominated, whereas in the former they are mostly structural.

As was mentioned above, in most of the frequency intervals there is a clear difference between the sound pressure levels associated with the modified models. For example, one of such intervals is between 200 and 300 Hz, where the difference of about 10 dB occurs between the graphs (0.002 and 0.005 m, and 0.005 and 0.008 m). Obviously, the increase in bottom plate thickness is one of the most efficient and easiest ways of reduction of road-induced structure-borne vehicle interior noise. However, this result comes at a price of increasing the overall mass of a vehicle, which is not always acceptable.

4. EFFECT OF MATERIAL VARIATIONS

So far, it was assumed that all the models under consideration have been made of steel plates. Real vehicles, however, have a number of panels made of different materials, including such as glass and plastics. For that reason, in this section we investigate the effects of changing materials of the windscreens and back-screens on generated structure-borne noise. The material changes are from steel to glass. The glass material characteristics are as follows: glass – Young's modulus $E = 7.2 \times 10^{10}$ N/m^2, Poisson's ratio $\nu = 0.23$ and the mass density $\rho = 2400$ kg/m^3.

The material parameters of steel for the windscreen and back-screen have been replaced by the parameters of glass, and the sound pressure responses have been calculated at the driver's and passenger's ear positions. Figure 7 shows the calculated pressure frequency response functions at the driver's (a) and passenger's (b) ear positions for both steel and glass materials.

Analysing the results shown in Fig. 7, (a) and (b), one can conclude that replacing steel windscreens and back-screens in simplified vehicle models by glass ones does not have much influence on the calculated sound pressure responses at the driver's and passenger's ear positions. Therefore, taking into account real material characteristics of vehicle windows may be unnecessary for modeling purposes.

5. CONCLUSIONS

In the present paper, a comprehensive parametric analysis of structure-borne vehicle interior noise in a simplified model of vehicle compartment has been carried out using finite element packages MSC.Patran and MSC.Nastran. Some important geometrical parameters of the model, such as overall length, height, and windscreen angle as well as

thickness of the bottom plate, have been varied in order to determine their influence on the sound pressure frequency responses calculated at the driver's and passenger's ear positions. Furthermore, different material parameters have been used to model wind- and back-screens, and their effect on the interior noise has been analysed.

It has been found that the geometrical modifications considered in this study have little influence on the structural natural frequencies. However, they strongly affect the acoustic natural frequencies and normal modes as well as the resulting structural-acoustic pressure responses.

In contrast to the above-mentioned variations of the model geometrical shape, the increase in thickness of the bottom plate suppresses structure-born interior noise very efficiently almost over the entire frequency range.

The change in material parameters of windscreens and back-screens does not have much influence on generated structure-borne interior noise.

REFERENCES

Fulford, R.A. and Petersson, B.A.T., 2000, "Estimation of vibrational power in built-up systems involving box-like structures, part1: Uniform force distribution", *Journal of Sound and Vibration* **232(5)**, 877-895.

Georgiev, V.B., Krylov, V.V. and Winward, R.E.T.B., 2004, "Finite element calculations of structural-acoustic modes of vehicle interior for simplified models of motorcars", *Proceedings of InterNoise 2004,* Prague, Czech Republic (on CD).

Krylov, V.V., 2002, "Simplified analytical models for prediction of vehicle interior noise", *Proceeding of the International Conference on Noise and Vibration Engineering*, (ISMA 2002), Leuven, Belgium, Ed. P. Sas, Vol. 5, 1973-1980.

Krylov, V.V., Walsh, S.J. and Winward, R.E.T.B., 2003, "Modelling of vehicle interior noise at reduced scale", *Proceedings of Euronoise 2003*, Naples, Italy (on CD).

Liang, J. and Petersson, B.A.T., 2001, "Dominant dynamic characteristics of built-up structures", *Journal of Sound and Vibration* **247(4)**, 703-718.

Lim, T.C., 2000, "Automotive panel noise contribution modeling based on finite element and measured structural-acoustic spectra", *Applied Acoustics* **60**, 505-519.

Luo, J. and Gea, H.C., 2003, "Optimal stiffener design for interior sound reduction using a topology optimization based approach", *Journal of Vibration and Acoustics* **125**, 267-273.

Lyon, R.H., 1963, "Noise reduction of rectangular enclosures with one flexible wall", *Journal of the Acoustical Society of America* **35**, 1791-1797.

Marburg, S., Beer, H.-J, Gier, J., Hardtke, H.-J., Rennert, R. and Perret, F., 2002, "Experimental verification of structural-acoustic modeling and design optimization", *Journal of Sound and Vibration* **252(4)**, 591-615.

Nefske, D.J., Wolf, J.A. and Howell, L.J., 1982, "Structural-acoustic finite element analysis of the automobile passenger compartment: A review of current practice". *Journal of Sound and Vibration* **80**, 247-266.

Petyt, M., Lea, J. and Koopmann, G.H., 1976, "A finite element method for determining the acoustic modes of irregular shaped cavities", *Journal of Sound and Vibration* **45**, 495-502.

Pretlove, A.J., 1965, "Free vibrations of a rectangular panel backed by a closed rectangular cavity", *Journal of Sound and Vibration* **2**, 197-209.

Pretlove, A.J., 1966, "Forced vibrations of a rectangular panel backed by a closed rectangular cavity", *Journal of Sound and Vibration* **3**, 252-261.

Sung, S.H. and Nefske, D.J., 1984, "A coupled structural-acoustic finite element model for vehicle interior noise analysis", *J. Vibr., Acoust., Stress, Rel., Design, Trans. of the ASME* **106**, 314-318.

List of Figure Captions:

Figure 1. Geometry of the base model (a) and of its different geometrical modifications, including the changes: in windscreen angle (b), in height (c) and in length (d).

Figure 2: Sound pressure responses calculated at the driver's ear position for the first (solid curve, Model 1) and second variations (dash-dotted curve, Model 2) of the windscreen angle (a) and their difference (b).

Figure 3: Sound pressure responses calculated at the driver's ear position for the first (solid curve, Model 1) and third variations (dash-dotted curve, Model 3) of the windscreen angle (a) and their difference (b).

Figure 4: Sound pressure responses calculated at the driver's ear position for the three values of height (a): h = 1.0 m (solid curve), h = 0.9 m (dash-dotted curve) and h = 1.1 m (dashed curved); and the differences (b) between the plots for h = 1 m and h = 1.1 m (solid curve, Diff 1), and for h = 1.0 m and h = 0.9 m (dash-dotted curve, Diff 2).

Figure 5: Sound pressure responses calculated at the driver's ear position for the three values of length (a): L = 2.0 m (solid curve), L = 1.9 m (dash-dotted curve) and L = 2.1 m (dashed curve); and the differences (b) between the plots for L

= 2.0 m and L = 2.1 m (solid curve, Diff 1), and L = 2.0 m and L = 1.9 m (dash-dotted curve, Diff 2).

Figure 6: Sound pressure responses calculated at the driver's (a) and passenger's (b) ear positions for the three values of thickness of the bottom plate: 5 mm (solid curve), 2 mm (dash-dotted curve) and 8 mm (dashed curve).

Figure 7: Sound pressure responses calculated at the driver's (a) and passenger's (b) ear positions for the base model with steel (solid curve) and glass (dash-dotted curve) windscreens and back-screens.

Figures:

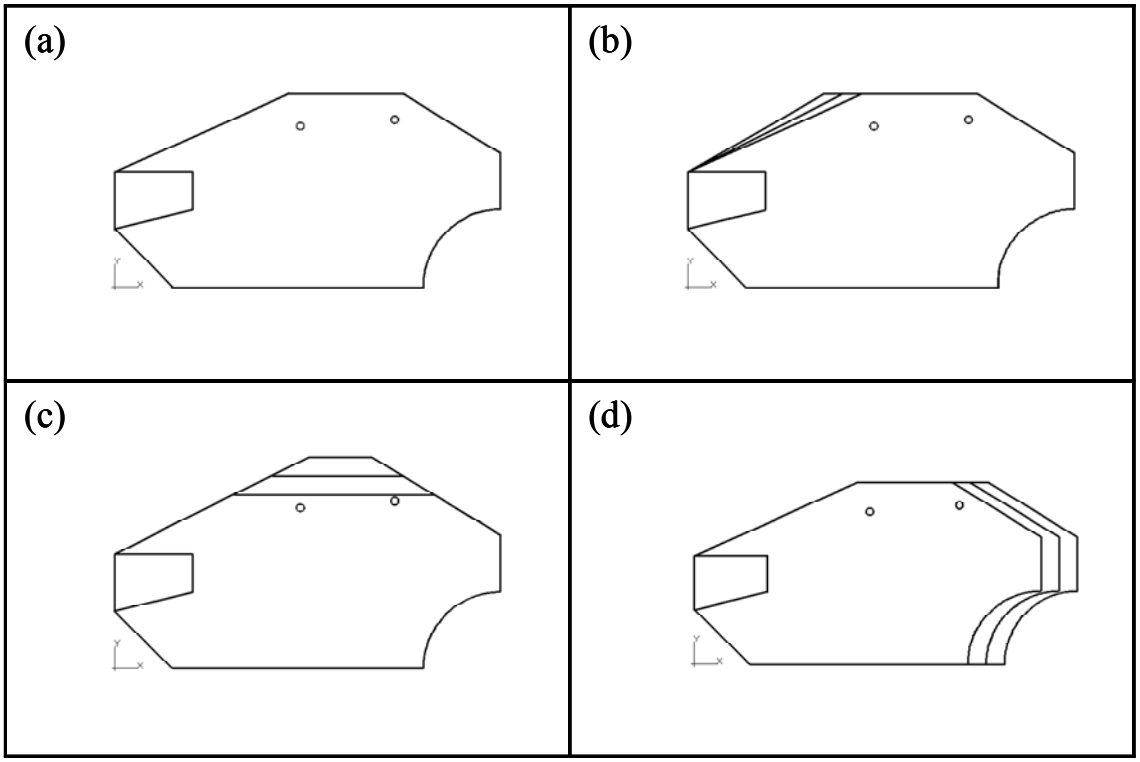

Figure 1. Geometry of the base model (a) and of its different geometrical modifications, including the changes: in windscreen angle (b), in height (c) and in length (d).

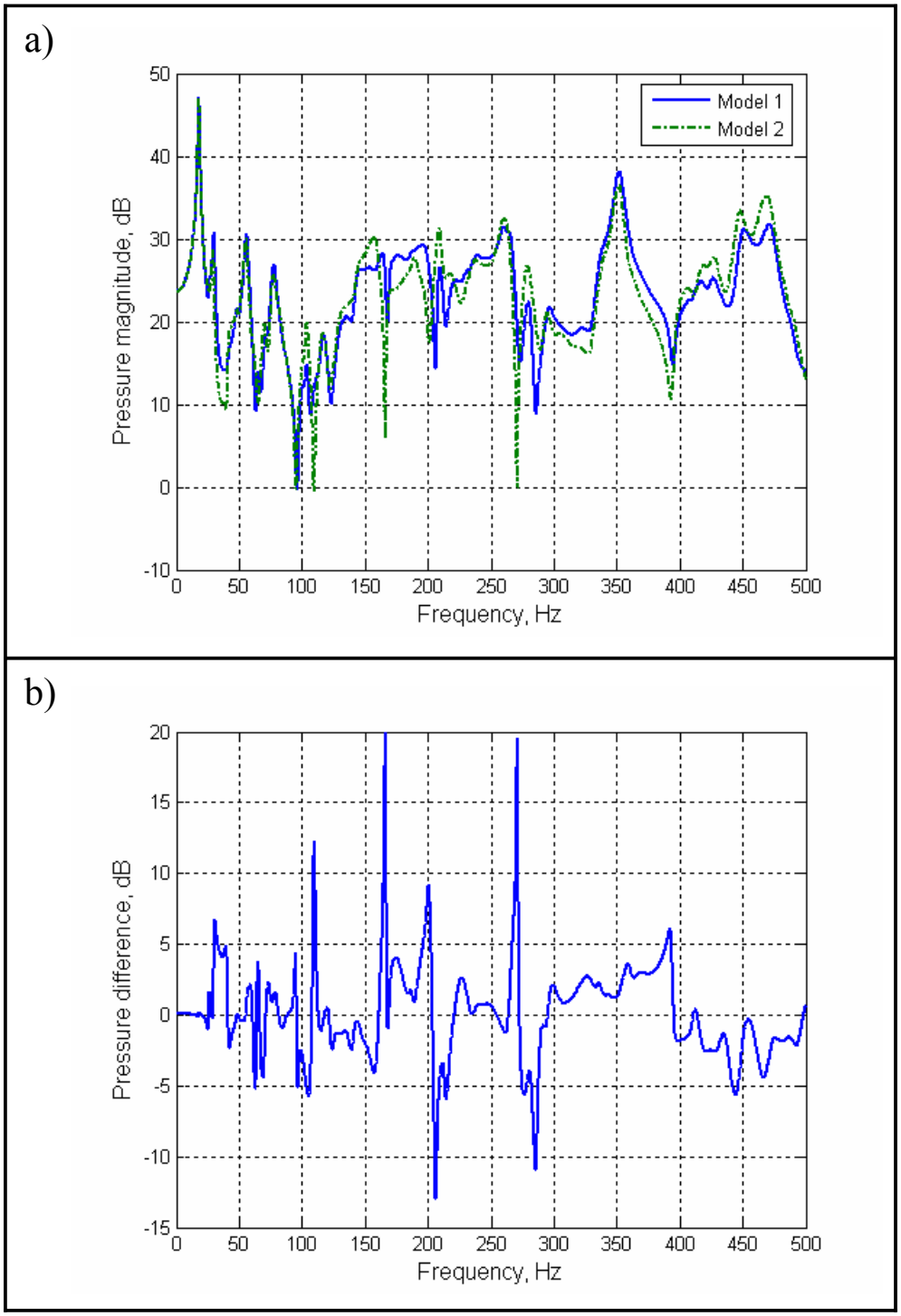

Figure 2: Sound pressure responses calculated at the driver's ear position for the first (solid curve, Model 1) and second variations (dash-dotted curve, Model 2) of the windscreen angle (a) and their difference (b).

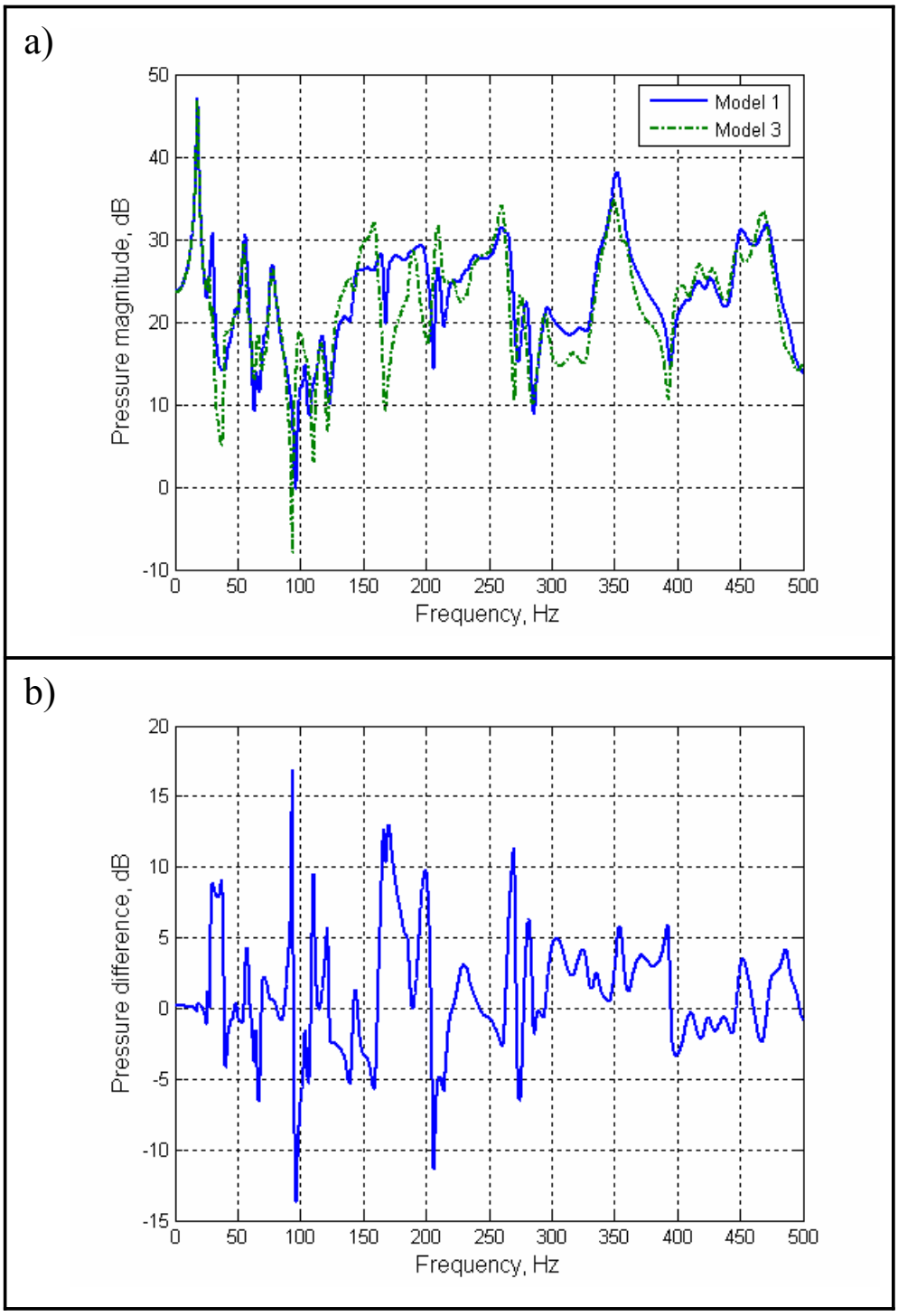

Figure 3: Sound pressure responses calculated at the driver's ear position for the first (solid curve, Model 1) and third variations (dash-dotted curve, Model 3) of the windscreen angle (a) and their difference (b).

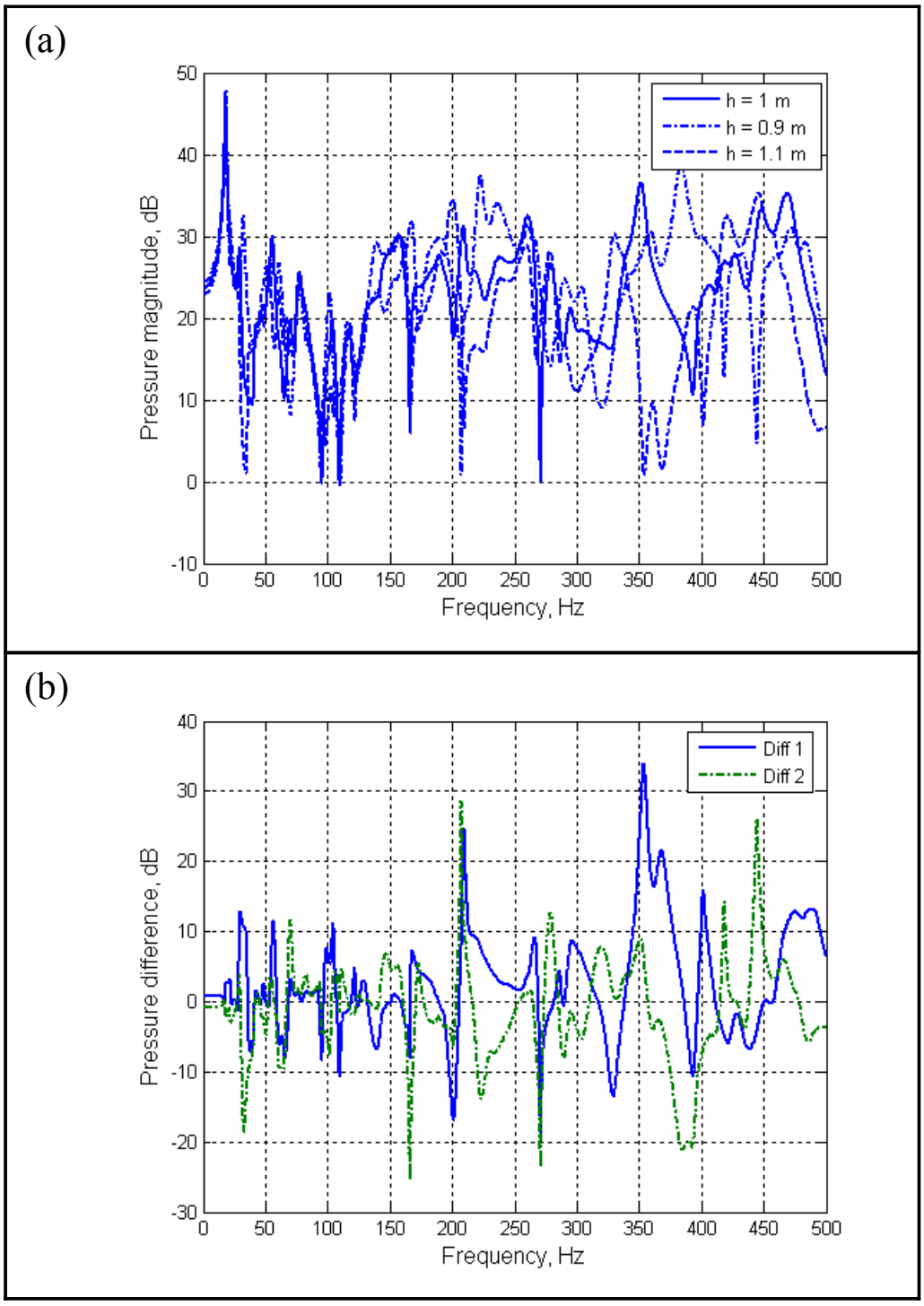

Figure 4: Sound pressure responses calculated at the driver's ear position for the three values of height (a): h = 1.0 m (solid curve), h = 0.9 m (dash-dotted curve) and h = 1.1 m (dashed curved); and the differences (b) between the plots for h = 1 m and h = 1.1 m (solid curve, Diff 1), and for h = 1.0 m and h = 0.9 m (dash-dotted curve, Diff 2).

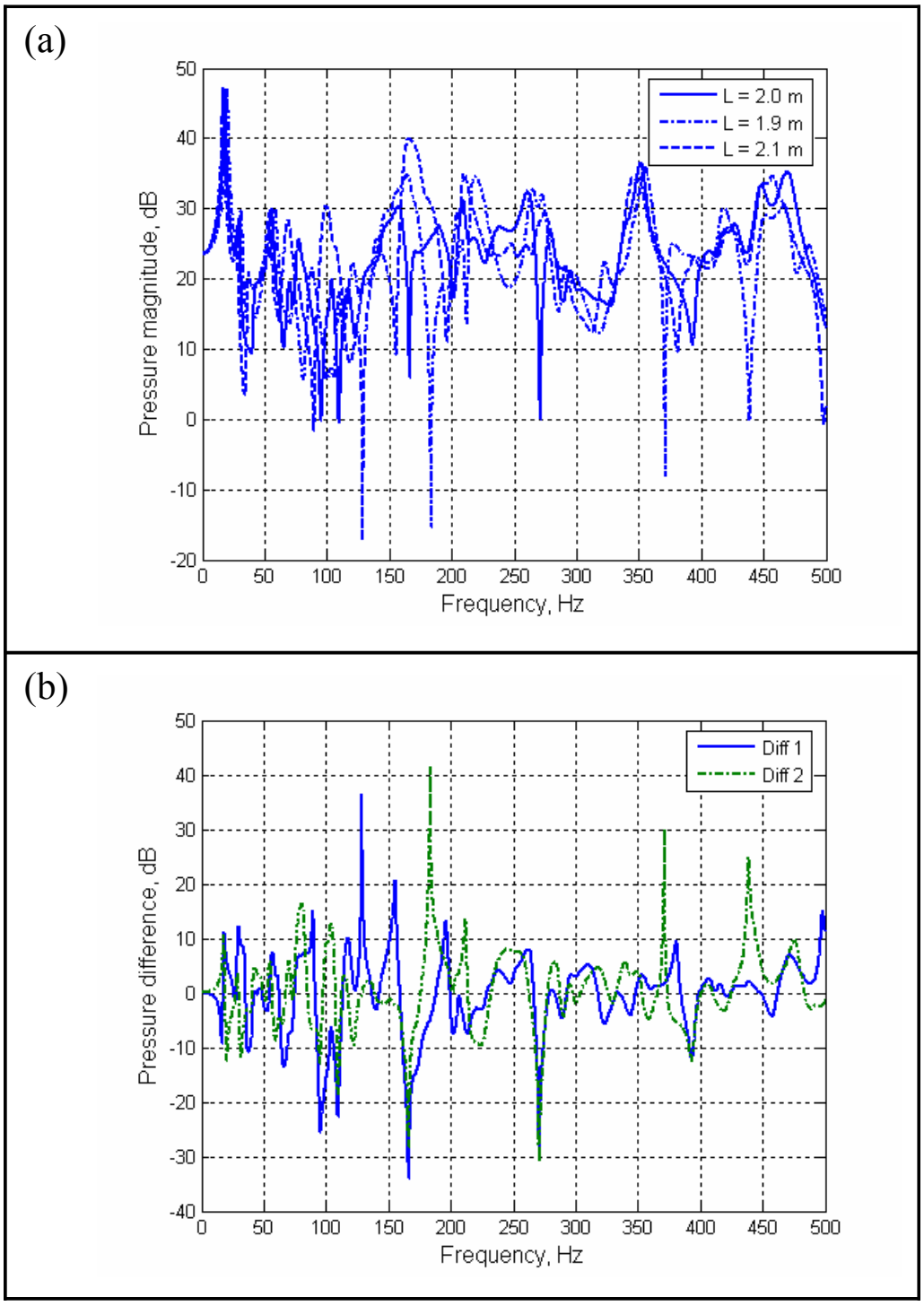

Figure 5: Sound pressure responses calculated at the driver's ear position for the three values of length (a): L = 2.0 m (solid curve), L = 1.9 m (dash-dotted curve) and L = 2.1 m (dashed curve); and the differences (b) between the plots for L = 2.0 m and L = 2.1 m (solid curve, Diff 1), and L = 2.0 m and L = 1.9 m (dash-dotted curve, Diff 2).

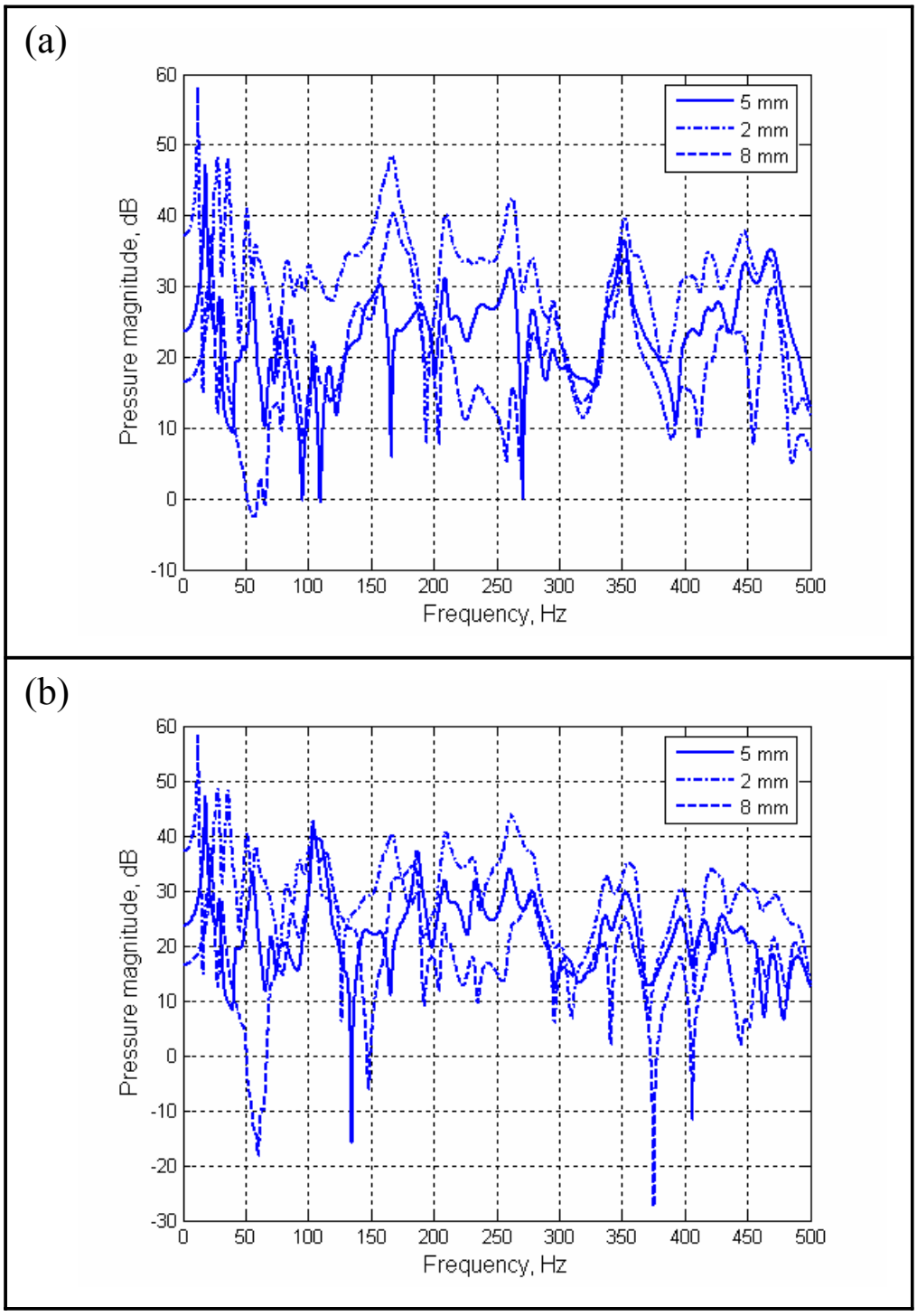

Figure 6: Sound pressure responses calculated at the driver's (a) and passenger's (b) ear positions for the three values of thickness of the bottom plate: 5 mm (solid curve), 2 mm (dash-dotted curve) and 8 mm (dashed curve).

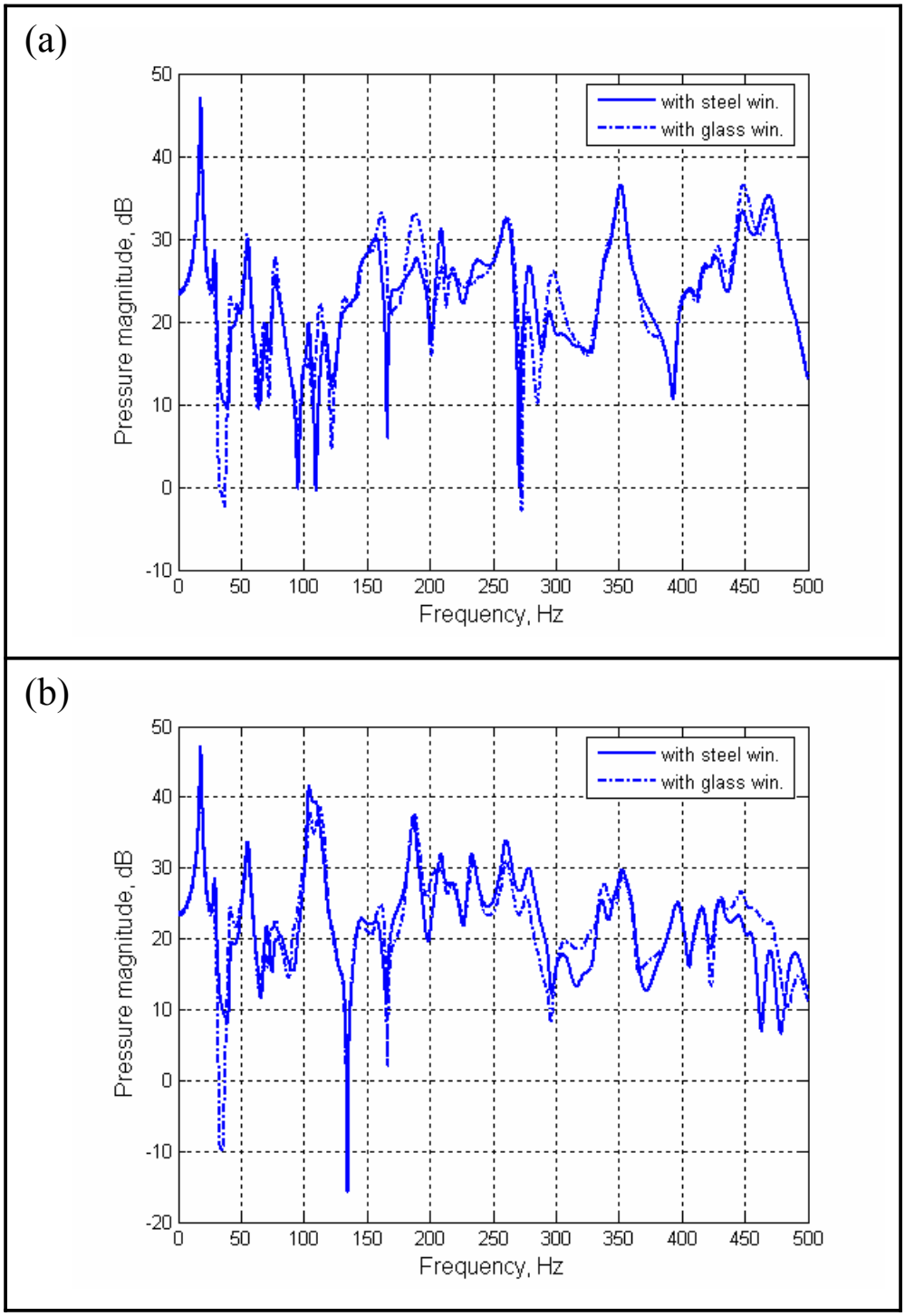

Figure 7: Sound pressure responses calculated at the driver's (a) and passenger's (b) ear positions for the base model with steel (solid curve) and glass (dash-dotted curve) windscreens and back-screens.